...p Physiol B (1991) 161:413–418

Machado et al 1991

Journal of Comparative Physiology B Biochemical, Systemic, and Environmental Physiology

...tudies on chitin and calcification in the inner layers ...f the shell of *Anodonta cygnea*

...Machado[1]*, M.L. Reis[2], J. Coimbra[1], and C. Sá[3]

...epartment of Physiology, Institute of Biomedical Sciences "Abel Salazar",
...aboratory of Geology and Mining of Oporto,
...epartment of Electrical Engineering, Faculty of Engineering, University of Oporto, Portugal

...cepted March 12, 1991

...ummary. An orthorhombic structure α-chitin, probably ...the form of a chitin-protein complex, was identified in ...e matrix of the shell of *Anodonta cygnea* by X-ray ...ffraction. Aragonite crystals of pseudohexagonal sym...etry were also found by a Lauegram on the nacreous ...yer of the shell. The orthorhombic structure of these ...o compounds together with the identical reticular ...pacing d_{110} corroborate, in *Anodonta cygnea*, the in...irect chitin-aragonite relationships already suggested ...r molluscan shells.

Observations with SEM in the inner surface of the ...hell showed $CaCO_3$ crystals with irregular geometrical ...hapes in spring and summer and regular geometrical ...hapes in autumn and winter. The more elaborate aspect ...ppearing in winter corresponds to an accurate hex...gonal shape. This suggests that the observed variability ...ay depend on the balance between calcium and hy...drogen ions in the extrapallial fluid.

Key words: Chitin – Aragonite – Calcification – Crystal...ne shape – *Anodonta cygnea*

Introduction

Biomineralization of the organic matrix of the molluscan ...hell has been the subject of many reviews. Wilbur, the ...primary proponent of the epitaxy theory, suggested that ...he matrix had an important regulatory role in shell ...formation (Wilbur 1976, 1984; Wilbur and Simkiss 1979). The crystal growth, mediated by an underlying ...tructural matrix, is a basic mode of skeletal formation ...dopted by many different organisms (Lowenstam 1981). ...According to Degens (1976), Weiner (1979), and Weiner and Traub (1981) the calcophilic matrix is composed of two structural units: a carrier-insoluble protein (chitinoproteic complex) of pleated sheets to which another acidic soluble unit, called mineralizing matrix with a strong affinity for calcium ions, was bound.

Studies by Beedham (1954) and Machado et al. (1988a) revealed the presence of chitin in the organic matrix of the shell of *A. cygnea*. Other works by Coimbra et al. (1988) and Machado et al. (1988b, 1988c, 1989, 1990a, 1990b) showed a strong chitin-calcification relationship and an interesting ion transport mechanism through the outer mantle epithelium (OME) which may greatly affect the calcification process.

This work emphasizes some chitin-aragonite relationships in the nacreous layer of *A. cygnea*. The study of the evolution of a crystalline shape by a correlation with the very recently published data (Coimbra et al. 1988; Machado et al. 1988a, 1988b, 1988c, 1989, 1990a, 1990b) is also described in order to understand the calcification mechanism.

Materials and methods

Freshwater clams *(Anodonta cygnea)* were collected from the Lagoon of Mira in Northern Portugal and kept in tanks at room temperature.

X-ray diffraction studies of superimposed pellicles (organic matrix) removed from the inner shell surface of several animals were carried out with a Debye-Scherrer powder camera of 11.4 cm diameter using the Straumanis arrangement. A Philips power supply PW 1130/00, operated at 40 kV and 20 mA (monochromatic Rad. Cukα by Ni filter) was also used. Two incident-beam directions were applied for 10–12 h: one parallel and another perpendicular to the sample surface. Rolled pellicles were also used in order to obtain a spectrum by sample rotating. The aragonite identification was obtained by calculation of the reticular distances from the X-ray diffraction patterns and checking them with the Powder Diffraction Data File. The chitin identification was obtained by calculation of the reticular distances from the X-ray diffraction patterns and checking them with calculated data from parameters of the chitobiose (orthorhombic unit cell; $a_0 = 4.76$ Å; $b_0 = 10.28$ Å; $c_0 = 18.85$ Å) according to Carlstrom (1957) and Rudall (1963),

...bbreviations: *OME* outer mantle epithelium; *SEM* scanning elec...ron microscopy

* To whom offprint requests should be sent

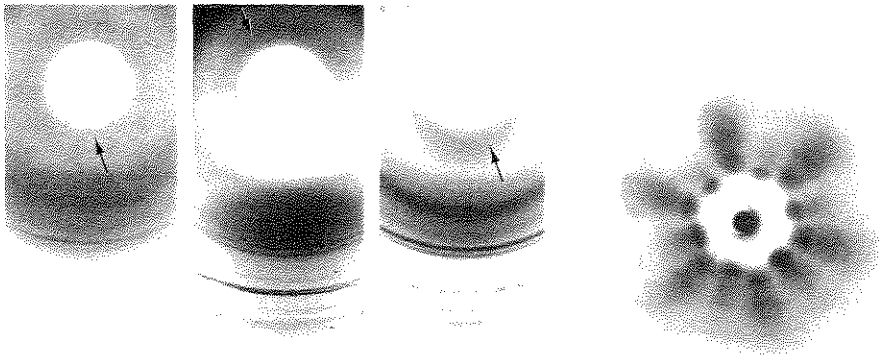

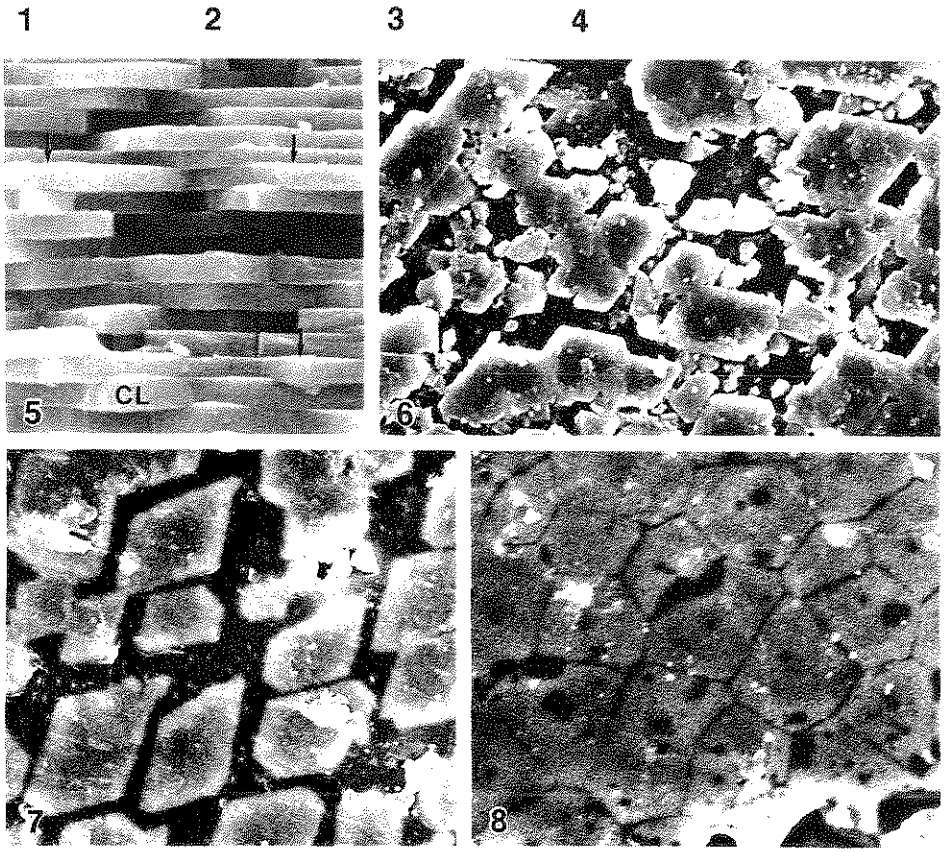

Figs. 1 and 2. X-ray diffraction spectrum, with a Debye-Scherrer powder camera, of soft chitinous pellicles removed from the inner shell surface of *A. cygnea*. The incident beam is, respectively, perpendicular (1) and parallel (2) to the pellicles. The reticular spacing and their indices are shown in A and B Table 1. Chitin band *(arrow)*

Fig. 3. X-ray diffraction spectrum, with a Debye-Scherrer powder camera, of soft chitinous pellicles removed from the inner shell surface of *A. cygnea*. The pellicles were submitted to a rotation movement. In this spectrum the chitinobiose unit reflection (10.3 Å) is evident. Chitin band *(arrow)*

Fig. 4. X-ray diffraction spectrum of nacreous layer of the shell, with the flat-camera technique, shows a pseudohexagonal structure in *A. cygnea*. The spots result from the reflections of specific crystallographic planes of aragonite monocrystals. The reticular spacing from reflection planes are shown in Table 3

Fig. 5. Observation (SEM) of a fractured section of the shell nacreous layer in *A. cygnea*. Calcareous lamellae (CL). Interlamellar space *(arrows)*. (× 18000)

Fig. 6. Inner growth surface of *A. cygnea* showing (SEM) rhombohedral crystals with some irregular and rough aspect in May (× 15000)

Fig. 7. Inner growth surface of *A. cygnea* showing (SEM) rhombohedral crystals in June. The poorly-stained image of the crystals is due to the presence of a layer of organic pellicle (× 15000)

Fig. 8. Inner growth surface of *A. cygnea* showing (SEM) crystals with irregular shapes in July and August. The poorly-stained image of crystals is due to the presence of a layer of organic pellicle (× 15000)

Table 1. Reticular spacing and respective indices of the α-chitin and aragonite of a soft mineralized pellicle. In **A** the incident beam is perpendicular (Fig. 1) and in **B** is parallel to the sample surface (Fig. 2)

	dA	hkl	Observation
A			
1	10.70	010	α-chitin*
2	5.50	013	α-chitin
3	4.60	101	α-chitin
4	4.30	110	aragonite + α-chitin
5	3.80	103	chitin
6	3.60	015	chitin
7	3.42	111	aragonite
8	3.28	021	aragonite
9	3.00	002	aragonite
10	2.72	121; 012	aragonite
11	2.50	200	aragonite
12	2.40	031	aragonite
13	2.34	112; 130; 022	aragonite
14	2.20	211	aragonite
15	2.12	220	aragonite
16	1.98	221	aragonite
17	1.88	041; 202	aragonite
18	1.82	132	aragonite
19	1.75	141; 113	aragonite
20	1.56	311	aragonite
21	1.51	232; 241	aragonite
22	1.48	321; 151	aragonite
23	1.42	312	aragonite
24	1.24	400	aragonite
B			
1	11.20	010	α-chitin*
2	5.40	013	α-chitin
3	4.30	110	aragonite + α-chitin
4	3.46	015	α-chitin
5	3.38	111	aragonite
6	3.23	021	aragonite
7	2.86	002	aragonite
8	2.80	121	aragonite
9	2.74	012	aragonite
10	2.68	012	aragonite
11	2.55	200	aragonite
12	2.48	200	aragonite
13	2.43	200	aragonite
14	2.39	031	aragonite
15	2.34	112	aragonite
16	2.28	130; 022	aragonite
17	2.09	211; 220	aragonite
18	1.96	221	aragonite
19	1.88	041; 202	aragonite
20	1.79	141; 113	aragonite
21	1.74	231	aragonite
22	1.70	222	aragonite
23	1.39	312; 330	aragonite
24	1.35	114	aragonite
25	1.23	400	aragonite
26	1.21	134; 243; 062	aragonite
27	1.18	153; 162; 260	aragonite

* X-ray diffraction diagram of chitinous pellicles is very different from the diagram of purified chitin. The X-ray reflections are broad and ill-defined, but within the limits of accuracy, we define the indices of this "native chitin"

Table 2. Determination of reticular distances from reflection planes of the aragonite crystals in the nacreous layer, calculated from standard parameters of aragonite. The incident beam is perpendicular to the sample surface (Fig. 4)

dA	4.14	2.50	2.10	1.48	1.13
hkl	110	200	220	330	–

using the equation $\sin\Theta^2 = Ah^2 + Bk^2 + Cl^2$, where $A = (\lambda/2a_0)^2$; $B = (\lambda/2b_0)^2$; $C = (\lambda/2c_0)^2$ and where λ is a Cukα wavelength.

The nacreous layer of the shell was also examined by X-ray diffraction. The flat-film technique (Lauegram) by transmission was used with a Philips PW 1030 power supply operated also at 40 kV and 20 mA (Rad. Cukα). The sample was irradiated for 7–8 h by a perpendicular white X-ray beam after crossing a collimator of 0.5 mm diameter. The sample–film distance was about 40 mm.

Morphological studies were undertaken by observation of the inner central surface of the shell nacreous layer with a JEOL JSM–35C scanning electron microscope (SEM) operated at 25 kV. The shell fragments were mounted on SEM specimen stubs with conductive silver paint and coated with gold. The observations were made on shell fragments of three clams at different periods of the calcification cycle.

Results

The X-ray diffraction data, from a Debye-Scherrer camera by perpendicular and parallel incident beams to the surface of a soft mineralized cuticle-organic matrix (Figs. 1 and 2), are presented in Tables 1A and 1B, respectively. These tables show the parameters of the reticular planes of two compounds and their indices. The interpretation of this radiogram allowed us to identify α-chitin and aragonite in the matrix of the shell. The X-ray diffraction

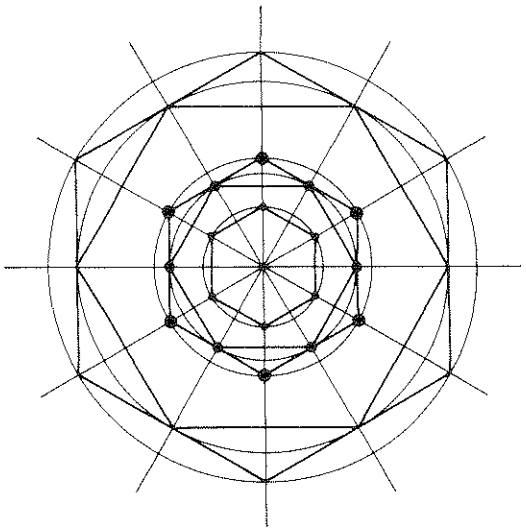

Diagram 1. This diagram emphasizes the pseudohexagonal symmetry of the aragonite observed in the Lauegram of the nacreous layer of the shell obtained by transmission on flat-film (Fig. 4). It suggests a structural arrangement of the chitobiose (orthorhombic unit cell) at different perpendicular planes to a hexagonal symmetry axis which is parallel to the incident X-ray beam; this fact seems according to the orientation and hexagonal morphology of the crystalline components observed in the scanning microphotographs.

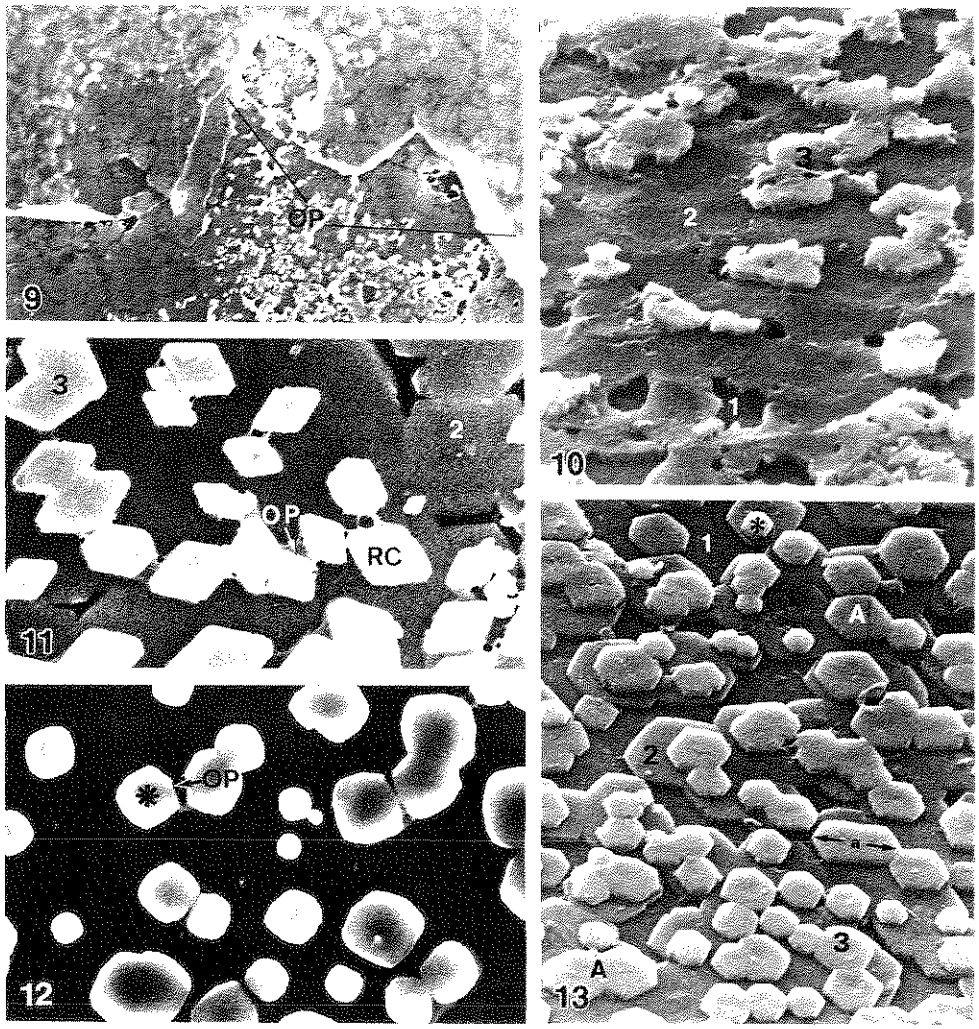

Fig. 9. Inner growth surface of *A. cygnea* showing (SEM) calcareous deposits with irregular shapes in September, covered by a thick organic pellicle indicated by a broken border line (OP). The upper region of this border line is less stained due to the pellicle (× 5000)

Fig. 10. A magnification (SEM) of the inner growth surface corresponding to the lower region of the border line (without pellicle), showing calcareous deposits with irregular shapes in September. Three distinct levels of calcification (1, 2, 3) are apparent (× 10000)

Fig. 11. Observation (SEM) of the inner surface in October and November showing rhombohedral crystals (RC) with very regular shapes. Some thin fragments of organic pellicle are present in the intercrystal spaces (OP). Three distint levels of calcification (1, 2, 3) are apparent (× 15000)

Fig. 12. Observation (SEM) of the inner surface in December showing transitory crystals but with regular shapes (*) also presenting thin fragments of organic pellicle in the intercrystal spaces (OP) (× 15000)

Fig. 13. Observation (SEM) of the shell inner face in winter (February) showing crystals with very elaborate regular shapes. Hexagonal crystal of aragonite (A) presenting lateral expansion are aligned with their a-axes (a) parallel to each other. Small crystal can be seen near the edge of the 001 face (*). Three distint levels of calcification (1, 2, 3) are apparent (× 10000)

diagram obtained by rotation movement of the sample (Fig. 3), clearly shows the reflection of the chitobiose unit with the characteristic period 10.3 Å. The data from Fig. 3 is not tabulated since it corresponds to Tables 1A and 1B.

The X-ray diffraction spectrum of the nacreous layer with a flat-camera shows aragonite crystals of a pseudo-hexagonal structure (Fig. 4 and Diag. 1). Halos, in radial directions, through the spots which defined the vertices of the hexagonal forms were also observed. These spots are due to the reflections of specific crystallographic planes of aragonite monocrystals (single crystals). The reticular spacing of the reflection planes and their indices are shown in Table 2.

Morphological observations (SEM) at high magnification, of nacreous layer of the shell, show two or three calcification levels (Figs. 6–13). Sections of the same layer show calcareous lamellae, each about 1 µm thick, separated by a very thin interlamellar spacing (Fig. 5) originated from organic pellicle. The organic matrix pellicle coating the calcareous layer reduces the image quality (Figs. 7–9) and can clearly be seen as an individualized structure (Fig. 9) or as small fragments (Figs. 11 and 12).

With regard to the morphology of the $CaCO_3$ crystals the central region of the shell, a great variability is apparent when the inner surface is observed in different months (Figs. 6–13). Figures 6–10 (May–September) show calcareous deposition with a gradually irregular geometrical shape. Figures 11–13 show that crystalline components with a regular geometrical shape are formed in the winter (October–February), with a hexagonal habit being the most elaborate shape (Fig. 13). The hexagonal crystals are elongated along the crystallographic axes and are orientated with their a-axes parallel to each other. Small crystals are seen on, or close to, the edges of the parent crystals on the 001 face (Fig. 13).

Discussion

The properties and proposed roles of organic matrices of calcified structures in organisms have been a matter of many recent studies (Watabe 1965; Crenshaw 1982; Krampitz et al. 1983; Mann 1983; Weiner et al. 1983; Roer and Dillaman 1984; Wilbur 1984). The matrix may act as an active surface to initiate crystal growth either by epitaxy or ionotropy (Greenfield et al. 1984; Weiner 1984; Wheeler and Sikes 1984; Wilbur 1984). In this way the matrix regulates and controls nucleation, polymorphic selection, crystal orientation, crystal growth, direction and/or crystal growth inhibition (Lowenstam 1981; Greenfield et al. 1984; Wheeler and Sikes 1984).

Chitin has recently been suggested as an important specific component of the molluscan organic matrix (Mann 1988). According to Poulicek et al. (1986), chitin does not seem to be directly related to the calcification process but is indirectly related to $CaCO_3$ metabolism, according to physiological and evolutionary evidence. This relationship is clearly supported by recent data (Machado et al. 1990a) which showed that an inhibition of chitin secretion causes disintegration of the calcareous layers.

The present results confirm the presence of chitin from the occurrence of several reflections, in addition to the reflection band 4.1–4.9 Å (100) already identified by Machado et al. (1988a). Thus, the 10.2 Å period (010) due to the chitobiose unit and the reticular spacing reflections (010; 013; 015; 135) correspond to the characteristic spectrum of α-chitin (orthorhombic). These results were obtained from the parameters indicated by Carlstrom (1957) and Ruddal (1963). The chitin reflection observed on our X-ray difractograms also has features suggesting that chitin must be associated with another compound, represented by a very large and a small delimited reflection. This compound could be protein, as found in other mollusc shells, and in insect and crustacean cuticles (Rudall 1963; Roer and Dillaman 1984; Poulicek et al. 1986).

Observations of the inner shell face with SEM clearly show crystals of hexagonal habit presenting a-axes oriented parallel to each other and growing simultaneously on two or three distinct levels. Lauegrams of the nacreous layer show that these are aragonite crystals with reflections of 4.14 Å (110), 2.50 Å (200), 2.10 Å (220), and 1.40 Å (330). There is also evidence of a pseudohexagonal monocrystalline structure resulting from an occasional association of aragonite crystals. Halos are also observed as a radial grouping of spots on the vertices of the hexagons from the central region. This results from components of the white radiation, present on the incident beam, which are reflected by deformed crystals (asterism).

The indirect chitin-aragonite relationship pointed out by Poulicek et al. (1986) is confirmed here by the orthorhombic structure of α-chitin and aragonite with parallel polymorphisms and an equal reticular spacing of the planes (110). The lamellar texture of these two compounds, which causes a little growth in the direction of lesser cohesion forces (001; Fraenkel and Rudall 1940, 1947), is also an indicator of this relationship. Pseudohexagonal symmetry was not demonstrated for chitin with present data. However, the spiral rotation relative to the chitin fibers, suggested by Roer and Dillaman (1984) and Mutvei (1974), means that a pseudohexagonal symmetry could be induced in the aragonite.

Although $CaCO_3$ crystallization on aragonite may be regulated by intrinsic properties of the organic matrix, the $CaCO_3$ crystal external habit is probably influenced by exogenous factors (Mutvei 1969; Wada 1970; Blackwell et al. 1977). Some exogenous factors recently identified (Coimbra et al. 1988; Machado et al. 1989, 1990b) may be important when speculating about the origins of the observed variability of crystalline forms, and also suggest a possible control mechanism. According to these authors the apical barrier of the outer mantle epithelium (OME) excretes H^+ towards the shell side regulating the pH of the extrapallial fluid, this excretion being greater during the October–December period. Thus, from October onwards the extrapallial fluid has an increased hydrogenion concentration which gradually induces an undersaturation of $CaCO_3$. However, a decrease in the calcium gradient through the OME in this period (Machado et al. 1988b) causes a reduction of calcium mobilization towards the extrapallial fluid. These two factors result in a very slow $CaCO_3$ deposition in the inner layer of the shell which makes the appearance of geometrical shape more and more regular and complex. It is in the winter that the more elaborate hexagonal habit is formed. Although the rate of hydrogen ion release is reduced in winter (Coimbra et al. 1988), the slow deposition is caused by a low calcium mobilization (Machado et al. 1988b) and low temperature. In contrast, more and more irregular geometrical shapes occur from spring onwards due to a gradual increase in the calcium gradient through the OME (Machado et al. 1988b), low hydrogen ion release (Coimbra et al. 1988), and high temperature inducing a fast deposition. This cyclic change of calcification rate agrees with observations by Poulicek et al. (1986) and Zandee et al. (1980) and parallels the seasonal fluctuations of energetic substrate in OME proposed by Machado et al. (1988c). Thus, according to Coimbra et al. (1988) the variability of crystalline shapes probably results mainly from a balance between calcium mobilization (subsquently HCO_3^-) and hydrogen

ion secretion through the OME towards the extrapallial fluid, inducing either slow crystallization (regular shapes) or fast crystallization (irregular shapes).

Acknowledgements. We thank JNICT (Junta Nacional de Investigação Científica e Tecnológica) for financial support.

References

Beedham GE (1954) Properties of the non-calcareous material in the shell of *Anodonta cygnea*. Nature 174:750

Blackwell JF, Gainey LF, Greenberg MJ (1977) Shell ultrastructure in two subspecies of the ribbed mussel, *Geukensia demissa* (Dillwyn 1817). Biol Bull 152:1–11

Carlstrom D (1957) The crystal structure of α-chitin. J Biophys Biochem Cytol 3:669–683

Coimbra J, Machado J, Ferreira KG, Ferreira HG (1988) The electrophysiology of the mantle of *Anodonta cygnea*. J Exp Biol 140:65–88

Crenshaw MA (1982) Mechanisms of normal biological mineralization of calcium carbonates. In: Nancollas GH (ed) Biological mineralization and demineralization. Springer, Berlin Heidelberg New York, pp 243–257

Degens ET (1976) Molecular mechanisms on carbonate, phosphate, and silica deposition in the living cell. Top Curr Chem 64:1–112

Fraenkel G, Rudall KM (1940) A study of the physical and chemical properties of the insect cuticle. Proc R Soc Lond Ser B 129:1–35

Fraenkel G, Rudall KM (1947) The structure of the insect cuticles. Proc R Soc Lond, Ser B 134:111–143

Greenfield EM, Wilson DC, Crenshaw MA (1984) Ionotropic nucleation of calcium carbonate by molluscan matrix. Am Zool 24:925–932

Krampitz G, Drolshagen H, Hausle J, Hof-Irmscher K (1983) Organic matrices of mollusc shells. In: Westbroek P, de Jong FW (eds) Biomineralization and biological metal accumulation. D. Reidel Publ. Co., Dordrecht Holland, pp 231–247

Lowenstam H (1981) Minerals formed by organisms. Science 211:1126–1131

Machado J, Castilho F, Coimbra J, Sá C, Monteiro E, Reis M (1988a) Ultrastructural and cytochemical studies in the mantle of *Anodonta cygnea*. Tissue Cell 20 (5):797–807

Machado J, Coimbra J, Sá C, Cardoso I (1988b) Shell thickening in *Anodonta cygnea* by induced acidosis. Comp Biochem Physiol 91A:645–651

Machado J, Ferreira KG, Ferreira HG, Coimbra J (1988c) Substrate activation of the short-circuit current of outer mantle epithelium of *Anodonta cygnea*. Comp Biochem Physiol 91A:487–492

Machado J, Coimbra J, Sá C (1989) Shell thickening in *Anodonta cygnea* by TBTO treatments. Comp Biochem Physiol 92C:77–80

Machado J, Coimbra J, Castilho, Sá C (1990a) Effects of diflubenzuron on shell formation of freshwater clam, *Anodonta cygnea*. Arch Environ Contam Toxicol 19:35–39

Machado J, Ferreira KG, Ferreira HG (1990b) The acid-base balance in the outer mantle epithelium of *Anodonta cygnea*. J Exp Biol 150:159–169

Mann S (1983) Mineralization in biological systems. Struct Bonding 54:125–174

Mann S (1988) Molecular recognition in the biomineralizat Nature 332:119–124

Mutvei H (1969) On the micro and ultrastructure of the conch in the nacreous layer of some recent and fossil molluscs. St holm Contrib Geol 20:1–17

Mutvei H (1974) SEM studies on arthropod exoskeletons. Par Decapod crustaceans, *Homarus gammarus* (L) and *Carc maenas* (L). Bull Geol Instn Univ Upsala, [N.S.], 4:73–80

Poulicek M, Voss-Foucart MF, Jeuniaux Ch (1986) Chitinopro complexes and mineralization in mollusc skeletal structures Muzzarelli RAA, Jeuniaux C, Gooday GW (eds) Chitin technol. [Proc. int. Conf. chitin chitosan]. Plenum Press, N York, pp 7–12

Roer R, Dillaman R (1984) The structure and calcification of crustacean cuticle. Am Zool 24:893–909

Rudall KM (1963) The chitin/protein complexes of insect cuticl In: Beament JWL, Treherne JE, Wigglesworth VB (eds) Adv ces in insect physiology. Academic Press, London New Yor vol. 1, pp 257–311

Zandee DI, Kluytmans JH, Zurburg W and Pieter H (1980) Se sonal variations in biochemical composition of *Mytilus edu* with reference to energy metabolism and gametogenesis. Net erlands J Sea Res 14(1):1–29

Wada K (1970) Studies on the calcified tissue in molluscs XV In: Yukawa H (ed) Profiles of Japanese science and scientis Kodansha Ltd., Tokyo, pp 226–244

Watabe N (1965) Studies on shell formation. XI. Crystalmatr relationships in the inner layers of mollusc shells. Ultrastruc Res 12:351–370

Weiner S (1979) Aspartic acid-rich proteins: major components the soluble organic matrix of mollusc shells. Calcif Tissue In 29:163–167

Weiner S, (1984) Organization of organic matrix components mineralized tissues. Am Zool 24:945–951

Weiner S, Traub W (1981) Organic-matrix-mineral relationship mollusc shell nacreous layers. In: Balaban M, Sussman J Traub W, Yong A (eds) Structural aspect of recognition an assembly in biological macromolecules. Balaban ISS, Rehov Philadelphia, pp 467–482

Weiner S, Traub W, Lowenstam HA (1983) Organic matrix i calcified exoskeletons. In: Westbroek P, de Jong EW (eds Biomineralization and biological metal accumulation. D. Reide Publ. Co., Dordrecht Holland, pp 205–224

Wheeler AP, Sikes CS (1984) Regulation of carbonate calcificatio by organic matrix. Am Zool 24:933–944

Wilbur KM (1976) Recent studies of invertebrate mineralizatio In: Watabe N, Wilbur KM (eds) The mechanisms of mineraliza tion in the invertebrates and plants. Univ. of South Carolin Press, Columbia, pp 74–108

Wilbur KM (1984) Many minerals, several phyla, and a few con siderations. Am Zool 24:839–845

Wilbur KM, Simkiss K (1979) Carbonate turnover and deposition by metazoa. In: Trudinger PA, Swaine DJ (eds) Biogeochemical cycling of mineral-forming elements. Elsevier, Amsterdam, pp 69–106